中国科学院高能物理研究所
Institute of High Energy Physics, Chinese Academy of Sciences

中国科学院大学
University of Chinese Academy of Sciences

Recent charmonium decay measurements at BESIII

Xueqiang Yan (IHEP, CAS, China)
On behalf of the BESIII Collaboration
yanxueqiang@ihep.ac.cn

43rd International Symposium on Physics in Collision (PIC 2024)

Oct 23, 2024, Athens, Greece

Outline

- **Introduction**
- **BESIII experiment**
- **Recent new measurements on charmonium decay**
  - Study of the $\chi_{cJ} \to \Lambda\bar{\Lambda}\phi$ decays
  - Study of the $\chi_{cJ} \to \Lambda\bar{\Lambda}\omega$ decays
  - Improved measurements of the branching fraction of $h_c \to \gamma\eta/\eta'$ and search for $h_c \to \gamma\pi^0$
  - Search for the radiative transition $\chi_{c1}(3872) \to \gamma\psi_2(3823)$
- **Summary**

Introduction

BESIII

Charmonium states are located in the transition region of perturbative and non-perturbative QCD

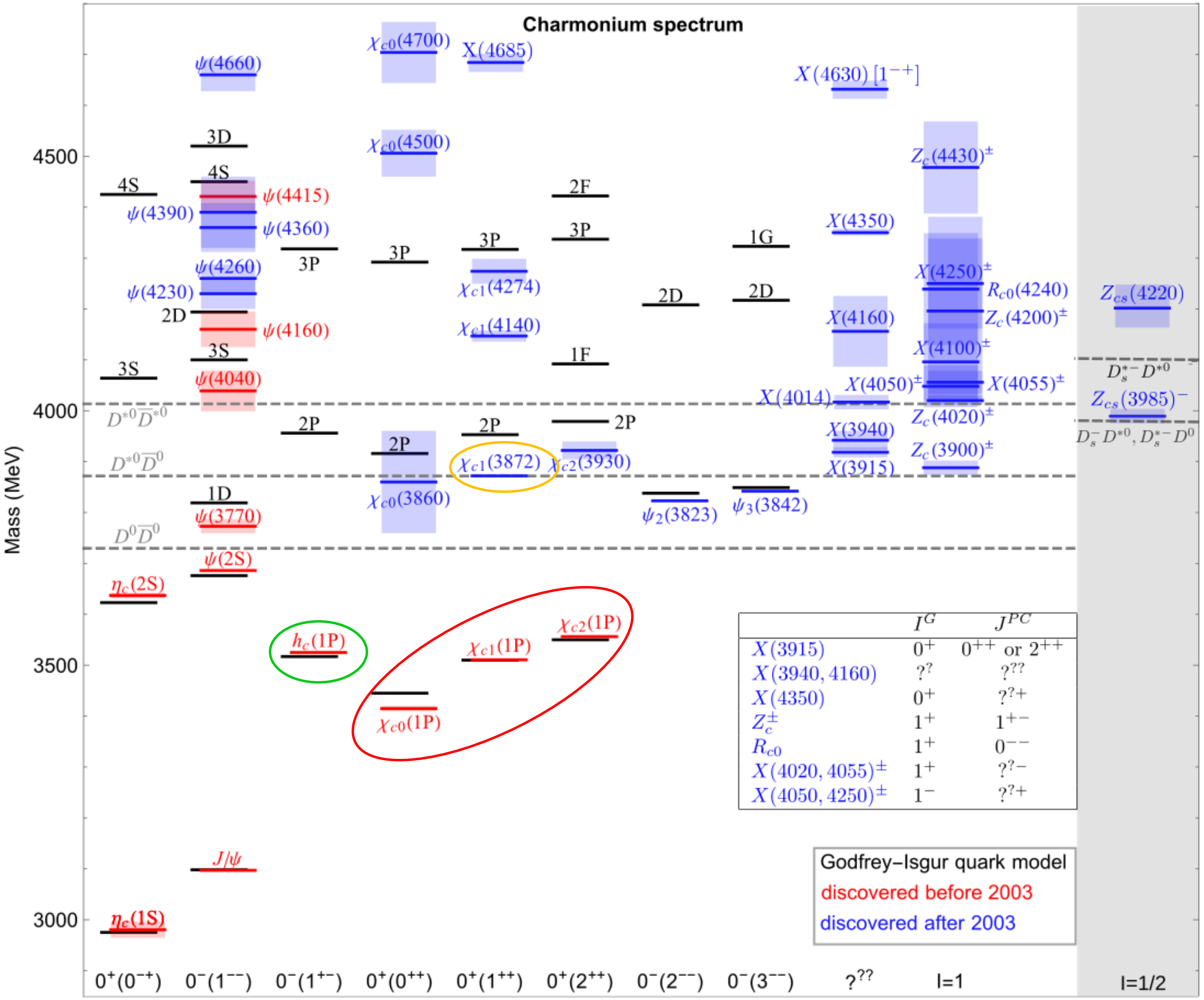

	I^G	J^{PC}
$X(3915)$	0^+	0^{++} or 2^{++}
$X(3940, 4160)$	$?^?$	$?^{??}$
$X(4350)$	0^+	$?^{?+}$
$Z_c^{\pm}$	1^+	1^{+-}
R_{c0}	1^+	0^{--}
$X(4020, 4055)^{\pm}$	1^+	$?^{?-}$
$X(4050, 4250)^{\pm}$	1^-	$?^{?+}$

- Theoretical studies indicate that the color octer mechanism may also influence the decays of the χ_{cJ}. Intensive measurements of χ_{cJ} hadronic decays are highly desirable to understand the underlying their decay dynamics.

- Excluding the E1 decay $h_c \to \gamma\eta_c$, the sum of the branching fractions of known h_c decay modes is only about 3%. Study of the radiative decays $h_c \to \gamma\ \eta/\eta'/\pi^0$ are particular desirable as these will provide more direct information on non-perturbative effects in heavy quarkonia.

- Charmonium states were supposed to be well described by nonrelativistic potential quark models. This was case before 2003, since the discovery of the $X(3872)$, also know as $\chi_{c1}(3872)$. It cannot be easily accommodated in the charmonium spectrum predicted in quark model. Classifying the charmonium-like structures may lead to insights into the confinement mechanism.

- Provide valuable insights to improve the understanding of the inner charmonium structure and test phenomenological mechanisms of non-perturbative QCD.

Beijing Electron Positron Collider (BEPCII)

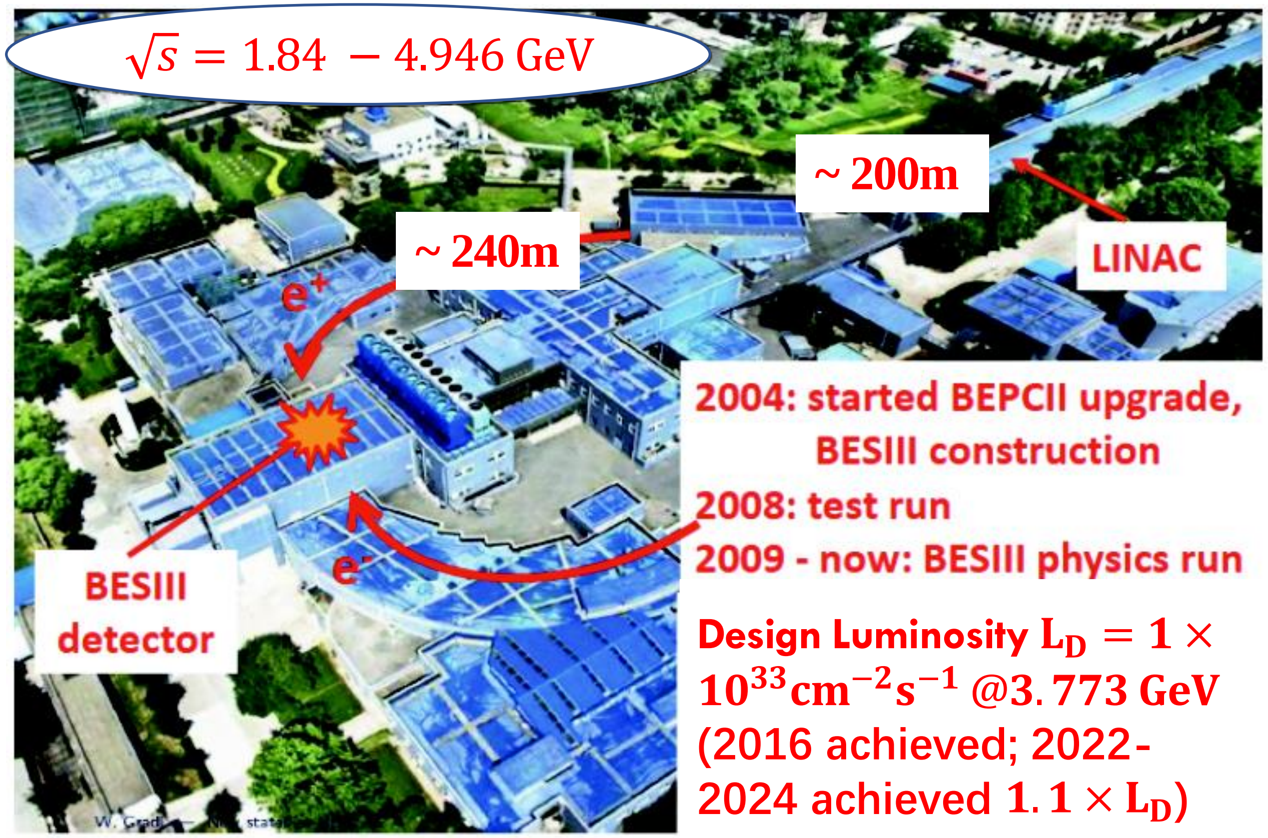

2004: started BEPCII upgrade, BESIII construction

2008: test run

2009 - now: BESIII physics run

Design Luminosity $L_D = 1 \times 10^{33} cm^{-2} s^{-1}$ @3.773 GeV (2016 achieved; 2022-2024 achieved $1.1 \times L_D$)

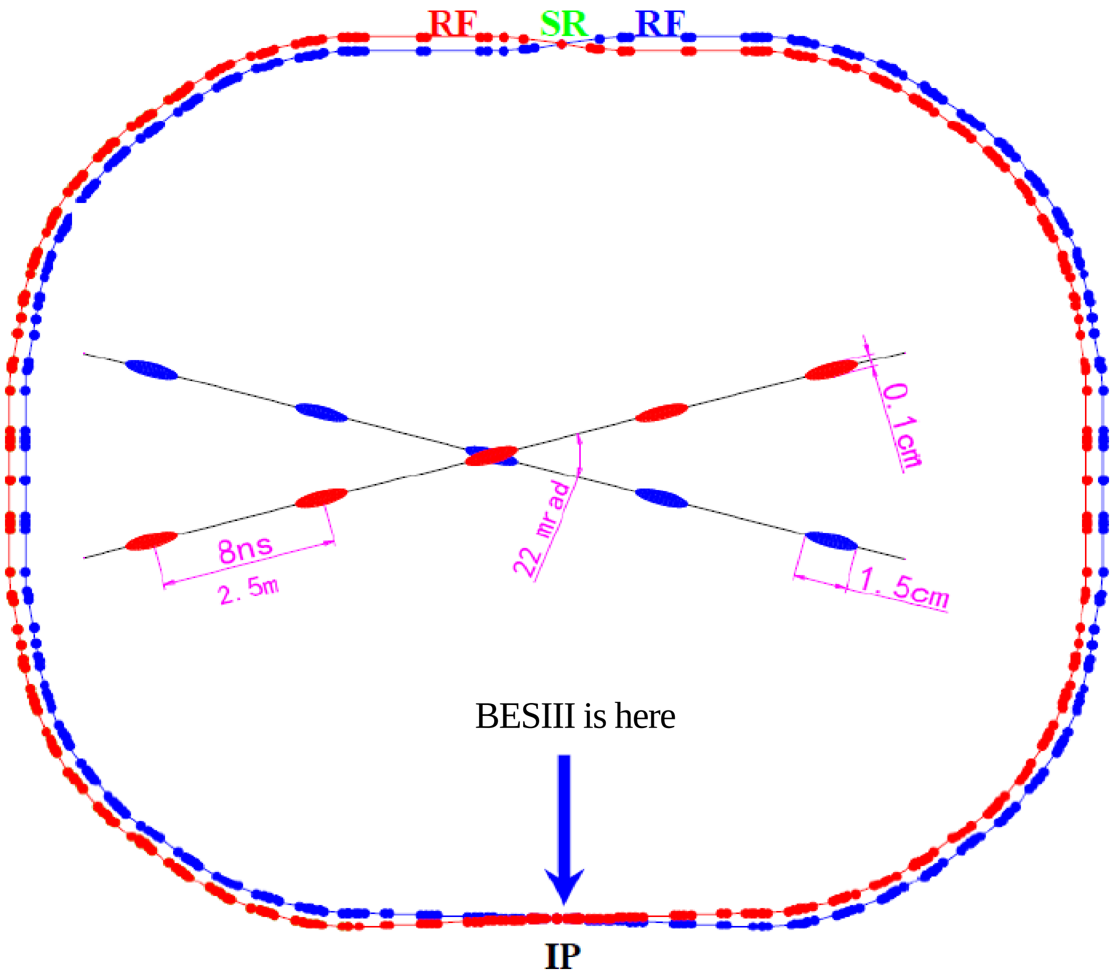

Beijing Spectrometer (BESIII)

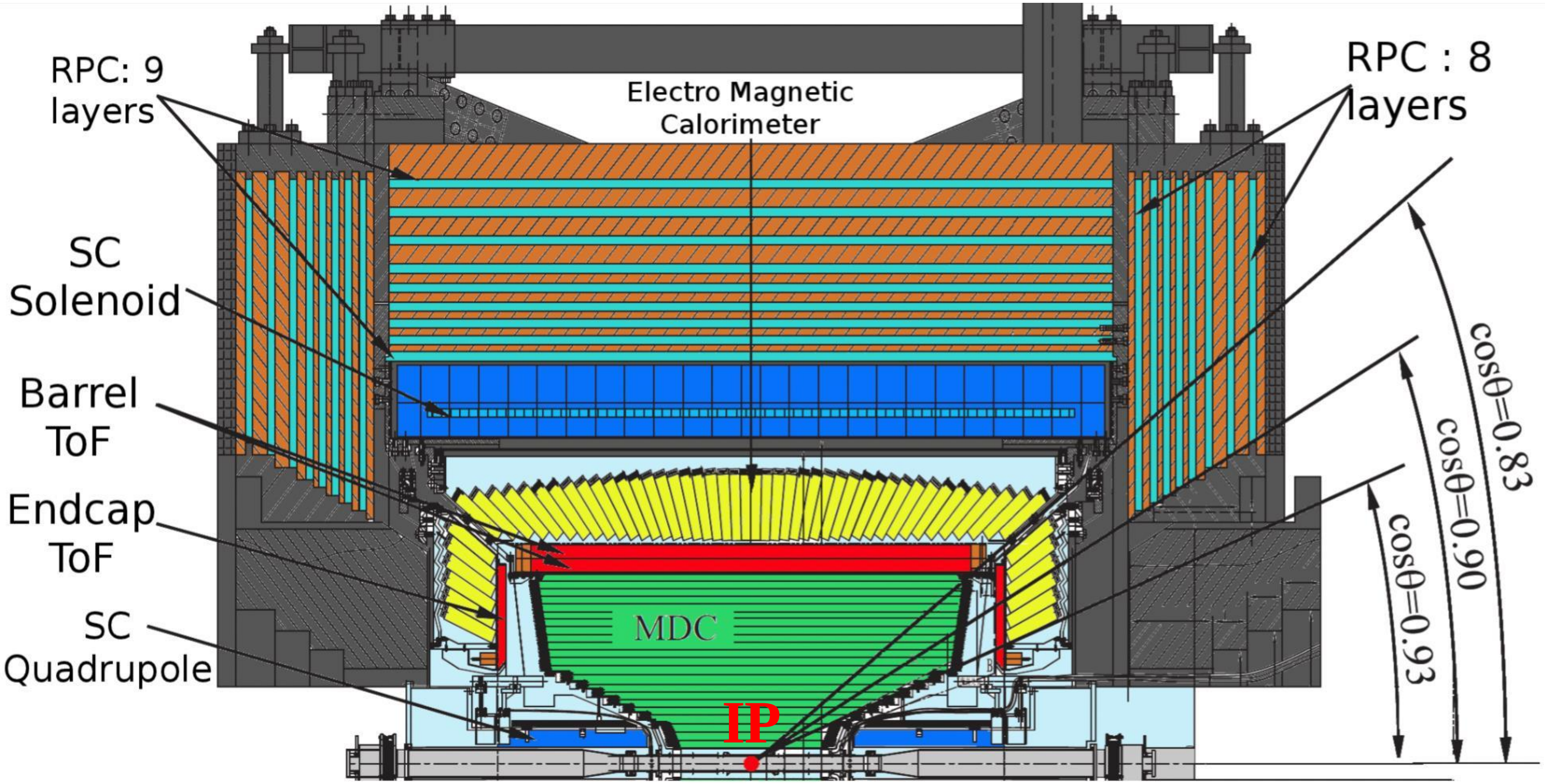

Multi-layer Drift Chamber

Single wire $\sigma_{r\phi}$(1 GeV)	130 μm
σ_z (1 GeV)	~2 mm
σ_z (1 GeV)	0.5 %
$\sigma_{dE/dx}$(1 GeV)	6%

Time of Flight Detector

σ_t	~68 ps (barrel)
	~60 ps (end cap)

EM Calorimeter

σ_E/E (1 GeV)	2.5%
Position resolution (1 GeV)	0.6 cm

Muon Detector

No. of layers (barrel/end cap)	9/8
Cut – off momentum	0.4 GeV/c

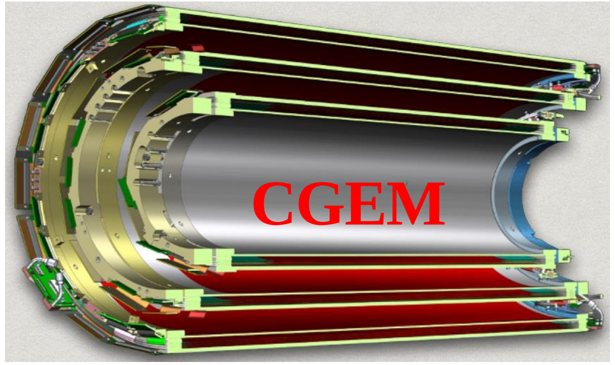

BESIII is replacing the inner part of the drift chamber with a three layers of CGEM detector, which has now been successfully extracted.

BESIII Dataset

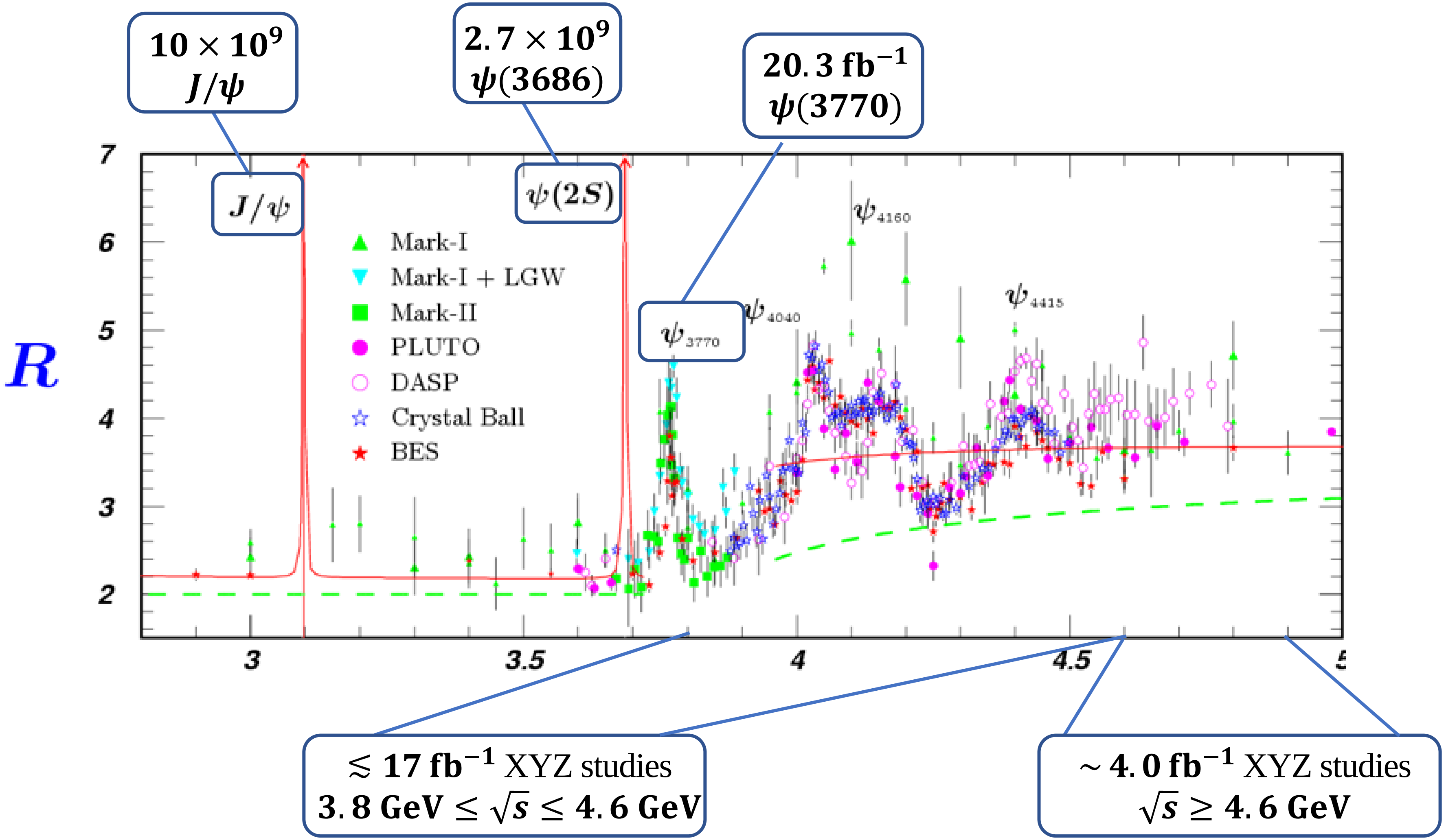

Recent new measurements on charmonium decay

- Study of the $\chi_{cJ} \to \Lambda\bar{\Lambda}\phi$ decays
- Study of the $\chi_{cJ} \to \Lambda\bar{\Lambda}\omega$ decays
- Improved measurements of the branching fraction of $h_c \to \gamma\eta/\eta'$ and search for $h_c \to \gamma\pi^0$
- Search for the radiative transition $\chi_{c1}(3872) \to \gamma\psi_2(3823)$

Study of the $\chi_{cJ} \to \Lambda\bar{\Lambda}\phi$ decays

Phys. Rev. D 110, 032016 (2024)

Using about 2.7 billion $\psi(3686)$ dataset

Search for the $\chi_{cJ} \to \Lambda\bar{\Lambda}\phi$ decays through the E1 transition $\psi(3686) \to \gamma\chi_{cJ}$ and determine the $\mathcal{B}(\chi_{cJ} \to \Lambda\bar{\Lambda}\phi)$

Fit to the $M(\Lambda\bar{\Lambda}\phi)$ at $[3.38, 3.60]$ GeV/c^2 to estimate the contributions.

	χ_{c0}	χ_{c1}	χ_{c2}
$N_{\rm obs}^{\chi_{cJ}}$	7.2 ± 3.0	51.6 ± 7.7	94.4 ± 10.7
Significance (σ)	4.1	11.3	13.0
$\varepsilon(\chi_{cJ} \to \Lambda\bar{\Lambda}\phi)$ (%)	0.45	1.61	2.54
$\mathcal{B}(\psi(3686) \to \gamma\chi_{cJ}) \cdot \mathcal{B}(\chi_{cJ} \to \Lambda\bar{\Lambda}\phi)(\times 10^{-6})$	$2.92 \pm 1.22 \pm 0.19$	$5.86 \pm 0.87 \pm 0.39$	$6.79 \pm 0.77 \pm 0.35$
$\mathcal{B}(\chi_{cJ} \to \Lambda\bar{\Lambda}\phi)(\times 10^{-5})$	$2.99 \pm 1.24 \pm 0.19$	$6.01 \pm 0.90 \pm 0.40$	$7.13 \pm 0.81 \pm 0.36$

First evidence

First observation

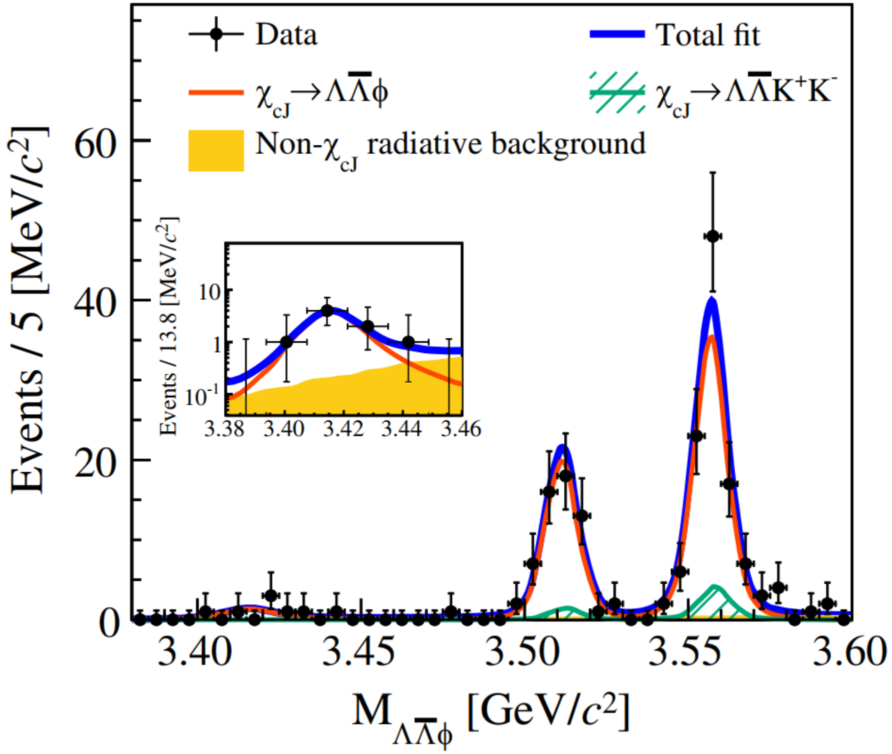

$$\mathcal{B}(\chi_{cJ} \to \Lambda\bar{\Lambda}\phi) = \frac{N_{obs}^{\chi_{cJ}}}{N_{\psi(3686)}\,\mathcal{B}(\psi(3686) \to \gamma\chi_{cJ})\mathcal{B}(\Lambda \to p\pi^-)\mathcal{B}(\bar{\Lambda} \to \bar{p}\pi^+)\mathcal{B}(\phi \to K^+K^-)\epsilon(\chi_{cJ} \to \Lambda\bar{\Lambda}\phi)} = \begin{cases} (2.99 \pm 1.24 \pm 0.19) \times 10^{-5} & \chi_{c0} \\ (6.01 \pm 0.90 \pm 0.40) \times 10^{-5} & \chi_{c1} \\ (7.13 \pm 0.81 \pm 0.36) \times 10^{-5} & \chi_{c2} \end{cases}$$

Stat. Syst.

Study of the $\chi_{cJ} \to \Lambda\bar{\Lambda}\omega$ decays

Phys. Rev. D 110, 032022 (2024)

Using about 2.7 billion $\psi(3686)$ dataset

Search for the $\chi_{cJ} \to \Lambda\bar{\Lambda}\omega$ decays through the E1 transition ($\psi(3686) \to \gamma\chi_{cJ}$) and determine the $\mathcal{B}(\chi_{cJ} \to \Lambda\bar{\Lambda}\omega)$

Simultaneous fit to the $M(\Lambda\bar{\Lambda}\omega)$ at [3.35, 3.60] GeV/c^2 in ω signal and sideband regions to estimate the contributions.

Decay	$N_{\rm fit}$	Significance	$\epsilon(\%)$	$\mathcal{B}(10^{-4})$
$\chi_{c0} \to \Lambda\bar{\Lambda}\omega$	316 ± 30	11.7σ	1.38	$2.37 \pm 0.22 \pm 0.25$
$\chi_{c1} \to \Lambda\bar{\Lambda}\omega$	202 ± 20	11.2σ	2.09	$1.01 \pm 0.10 \pm 0.11$
$\chi_{c2} \to \Lambda\bar{\Lambda}\omega$	251 ± 23	11.8σ	1.92	$1.40 \pm 0.13 \pm 0.17$

First observation

$$\mathcal{B}(\chi_{cJ} \to \Lambda\bar{\Lambda}\omega) = \frac{N_{fit}}{N_{\psi(3686)}\,\mathcal{B}(\psi(3686) \to \gamma\chi_{cJ})\mathcal{B}(\Lambda \to p\pi^-)\mathcal{B}(\bar{\Lambda} \to \bar{p}\pi^+)\mathcal{B}(\omega \to \pi^+\pi^-\pi^0)\mathcal{B}(\pi^0 \to \gamma\gamma)\epsilon} = \begin{cases} (2.37 \pm 0.22 \pm 0.25) \times 10^{-4} & \chi_{c0} \\ (1.01 \pm 0.10 \pm 0.11) \times 10^{-4} & \chi_{c1} \\ (1.40 \pm 0.13 \pm 0.17) \times 10^{-4} & \chi_{c2} \end{cases}$$

Stat. Syst.

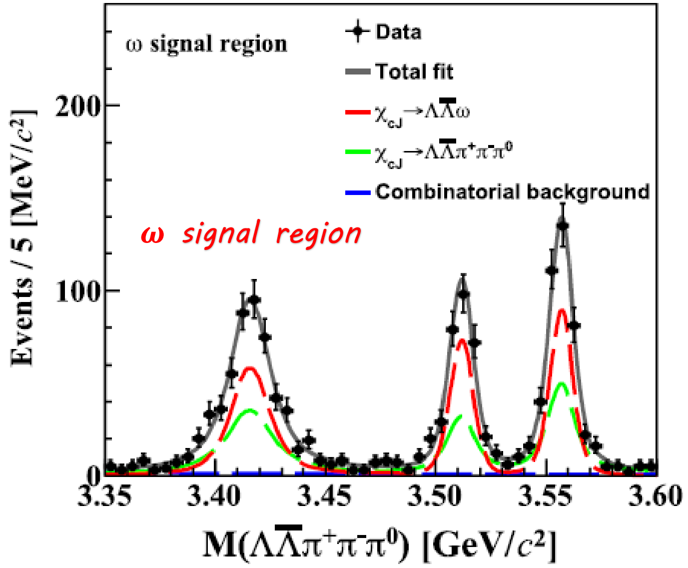

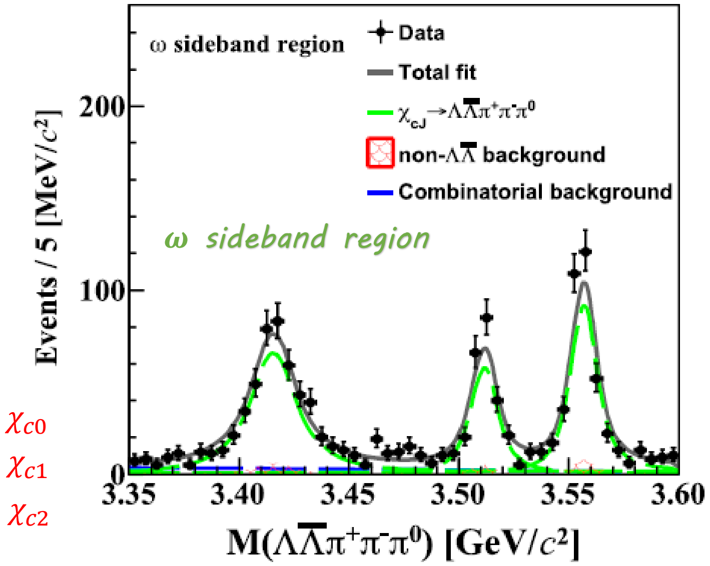

Study of the $h_c \to \gamma\, \eta/\eta'/\pi^0$ decays (1)

JHEP 2024, 180 (2024)

Using about 2.7 billion $\psi(3686)$ dataset

Search for the $h_c \to \gamma\, \eta/\pi^0$ decays through the $\psi(3686) \to \pi^0 h_c$, and determine the $\mathcal{B}(h_c \to \gamma\, \eta/\eta')$ and the upper limit of $\mathcal{B}(h_c \to \gamma\, \pi^0)$.

Simultaneous fit to the $M(\gamma\pi^+\pi^-\eta)$ and $M(\gamma\gamma\pi^+\pi^-)$ at $[3.46, 3.56]$ GeV/c^2 to estimate the $h_c \to \gamma\, \eta'$ contributions.

	$\mathscr{B}(h_c \to \gamma\eta')(\times 10^{-3})$
This work	$1.40 \pm 0.11 \pm 0.04 \pm 0.10$
BESIII [1]	$1.52 \pm 0.27 \pm 0.29$

$\mathcal{B}(\psi(3686) \to \pi^0 h_c)$

Stat. Syst.

$$\begin{cases} N^{sig}(\eta' \to \pi^+\pi^-\eta) = N^{tot} \cdot \mathcal{B}(\psi(3686) \to \pi^0 h_c)\mathcal{B}(\pi^0 \to \gamma\gamma)\boldsymbol{\mathcal{B}(h_c \to \gamma\eta')}\mathcal{B}(\eta' \to \pi^+\pi^-\eta)\mathcal{B}(\eta \to \gamma\gamma)\epsilon_{\pi^+\pi^-\eta} \\ N^{sig}(\eta' \to \gamma\pi^+\pi^-) = N^{tot} \cdot \mathcal{B}(\psi(3686) \to \pi^0 h_c)\mathcal{B}(\pi^0 \to \gamma\gamma)\boldsymbol{\mathcal{B}(h_c \to \gamma\eta')}\mathcal{B}(\eta' \to \gamma\pi^+\pi^-)\epsilon_{\gamma\pi^+\pi^-} \end{cases}$$

Common fit parameter

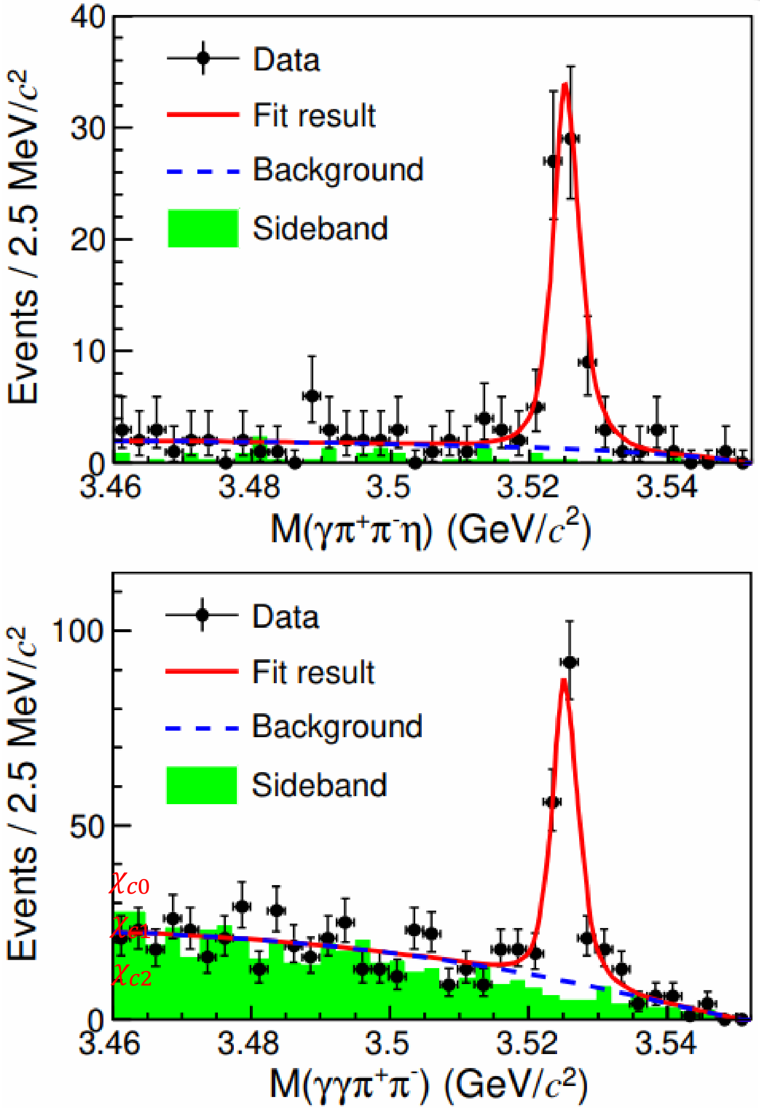

[1] Phys. Rev. Lett. **116**, 251802 (2016)

Study of the $h_c \to \gamma\, \eta/\eta'/\pi^0$ decays(2)

JHEP 2024, 180 (2024)

Simultaneous fit to the $M(\gamma\gamma\gamma)$ and $M(\gamma\pi^+\pi^-\pi^0)$ at [3.46 3.56] GeV/c^2 to estimate the $h_c \to \gamma\, \eta$ contributions.

9.0σ *First observation*

	$\mathcal{B}(h_c \to \gamma\eta)(\times 10^{-4})$
This work	$3.77 \pm 0.55 \pm 0.13 \pm 0.26$
BESIII [1]	$4.7 \pm 1.5 \pm 1.4$

Stat. Syst. $\mathcal{B}(\psi(3686) \to \pi^0 h_c)$

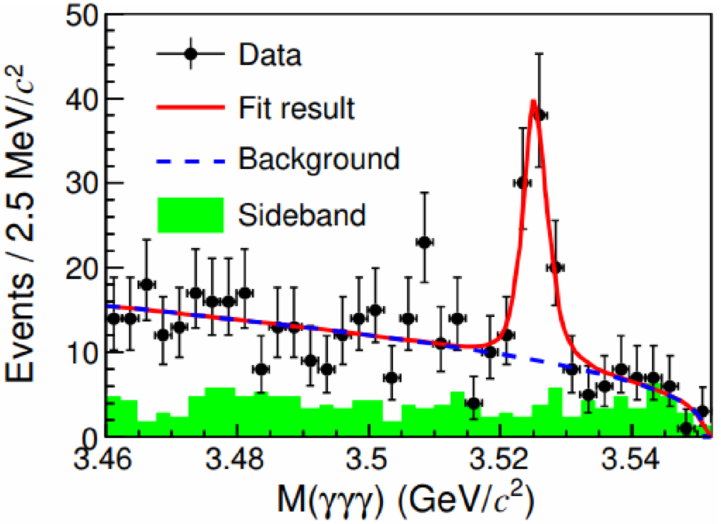

$$\begin{cases} N^{sig}(\eta \to \gamma\gamma) = N^{tot} \cdot \mathcal{B}(\psi(3686) \to \pi^0 h_c)\mathcal{B}(\pi^0 \to \gamma\gamma)\mathcal{B}(h_c \to \gamma\eta)\mathcal{B}(\eta \to \gamma\gamma)\epsilon_{\gamma\gamma} \\ N^{sig}(\eta \to \pi^+\pi^-\pi^0) = N^{tot} \cdot \mathcal{B}(\psi(3686) \to \pi^0 h_c)\mathcal{B}(\pi^0 \to \gamma\gamma)\mathcal{B}(h_c \to \gamma\eta)\mathcal{B}(\eta \to \pi^+\pi^-\pi^0)\mathcal{B}(\pi^0 \to \gamma\gamma)\epsilon_{\pi^+\pi^-\pi^0} \end{cases}$$

Common fit parameter

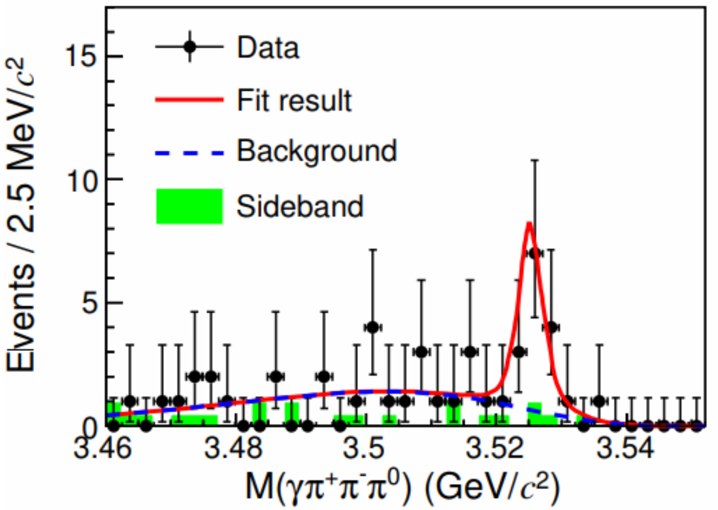

[1] Phys. Rev. Lett. **116**, 251802 (2016)

Study of the $h_c \to \gamma\, \eta/\eta'/\pi^0$ decays (3)

JHEP 2024, 180 (2024)

Fit to the $M(\gamma\pi^0)$ at [3.46 3.56] GeV/c^2 to estimate the $h_c \to \gamma\, \pi^0$ contributions.

No significant signal

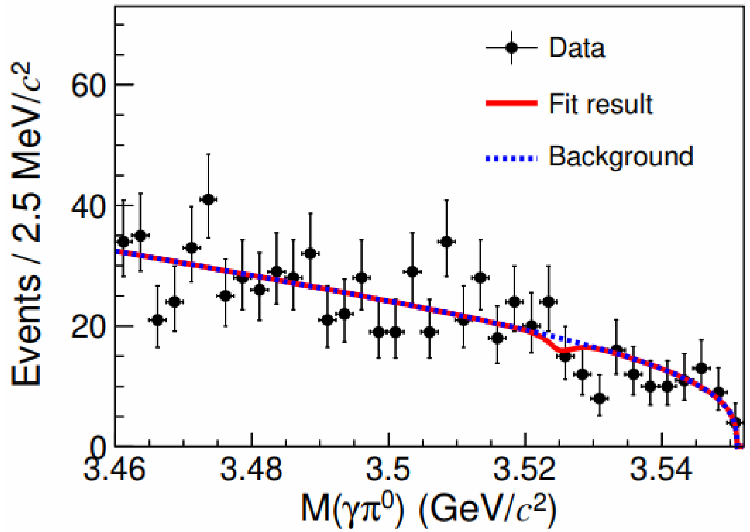

An upper limit of 5.0×10^{-5} is set on the $\mathcal{B}(h_c \to \gamma\pi^0)$ at the 90% confidence level.

Using a profile likelihood fit:

- Green solid line: The likelihood distribution incorporating additive systematic uncertainties
- Red dashed line: Convolution of thelikelihood curve with multiplicative systematic uncertainties

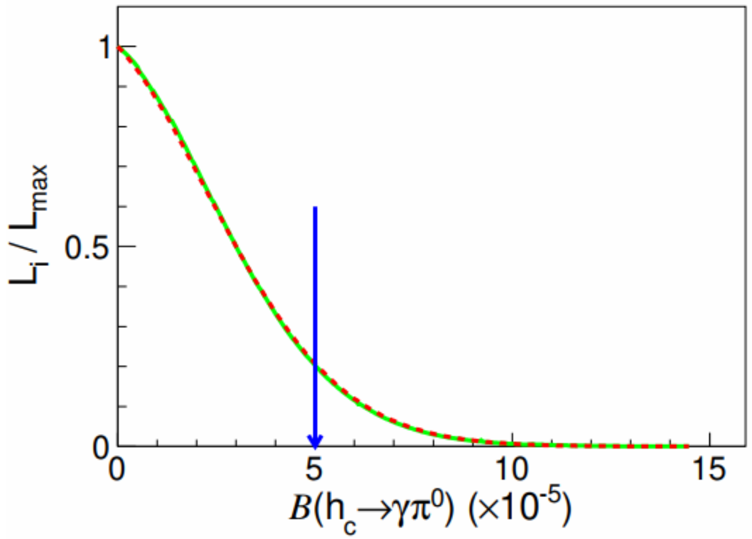

Search for the $\chi_{c1}(3872) \to \gamma\psi_2(3823)$ decay

Phys. Rev. D 110, 01201 (2024)

Using 15 energy points @$\sqrt{s} = [4.178, 4.278]$GeV ~ 9 fb^{-1}

Search for the radiative transition $\chi_{c1}(3872) \to \gamma\psi_2(3823)$, with $\psi_2(3823) \to \gamma\chi_{c1}$.

No $\chi_{c1}(3872) \to \gamma\psi_2(3823)$ events are found in the $M(\gamma\psi_2(3823))$ distribution.

$$\mathcal{R}_{\chi_{c1}(3872)} = \frac{N_{obs} - r \cdot N_{obs}^{sdb}}{N_{\pi^+\pi^-J/\psi} \cdot \frac{\epsilon_{\gamma\psi_2(3823)}}{\epsilon_{\pi^+\pi^-J/\psi}} \cdot \mathcal{B}(\chi_{c1} \to \gamma J/\psi)} < 0.075$$

@90% confidence level

More than 1σ below the theoretical calculations of $\mathcal{R}_{\chi_{c1}(3872)}$ under the assumption that the $\chi_{c1}(3872)$ is the pure charmonium state $\chi_{c1}(2P)$.

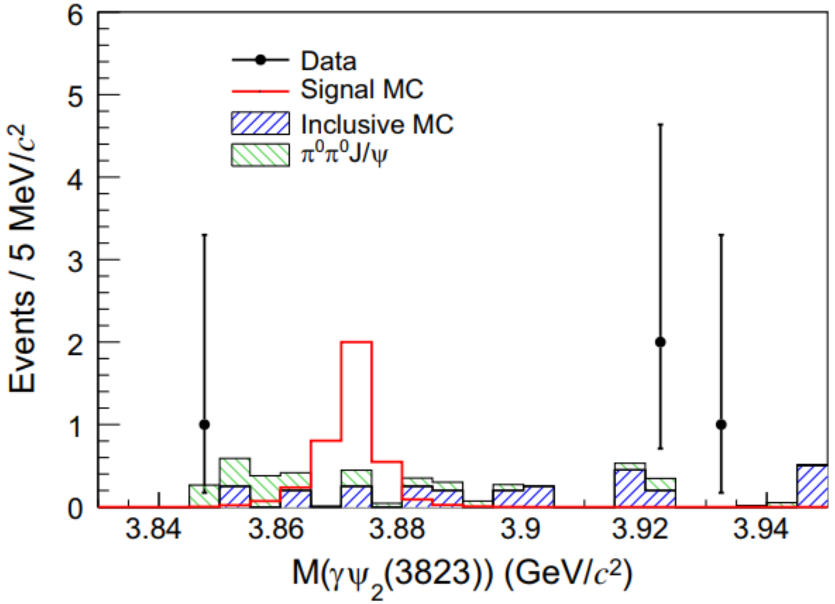

$$\mathcal{R}_{\chi_{c1}(3872)} \equiv \frac{\mathcal{B}(\chi_{c1}(3872) \to \gamma\psi_2(3823), \psi_2(3823) \to \gamma\chi_{c1})}{\mathcal{B}(\chi_{c1}(3872) \to \pi^+\pi^- J/\psi)}$$

$\Gamma_{\chi_{c1}(3872)} = 1190 \pm 210$ keV [1]
$\Gamma_{\psi_2(3823)} = 520 \pm 100$ keV [2]
$\mathcal{B}(\chi_{c1}(3872) \to \pi^+\pi^- J/\psi) = (3.8 \pm 1.2) \times 10^{-2}$ [1]

	NR [3]	GI [3]	LQCD [2]
$\Gamma_{\chi_{c1}(2P)\to\gamma\psi(1^3D_2)}$ (keV)	35	18	...
$\Gamma_{\psi(1^3D_2)\to\gamma\chi_{c1}(1P)}$ (keV)	307	268	337 ± 27
$\mathcal{R}_{\chi_{c1}(2P)}$	0.46 ± 0.19	0.21 ± 0.09	0.50 ± 0.21, 0.26 ± 0.11

[1] Prog. Theor. Exp. Phys. **2022**, 093C01 (2022)
[2] Phys. Rev. D **109**, 014513 (2024)
[3] Phys. Rev. D **72**, 054026 (2005)

Summary

- BESIII has achieved significant process in the study of charmonium decay
  - First observation of $\chi_{c1,2} \to \Lambda\bar{\Lambda}\phi$ and first evidence of $\chi_{c0} \to \Lambda\bar{\Lambda}\phi$
  - First observation of $\chi_{cJ} \to \Lambda\bar{\Lambda}\omega$
  - Improved measurements of $\mathcal{B}(h_c \to \gamma\eta/\eta')$ and give the upper limit of $h_c \to \gamma\pi^0$
  - Give the upper limit of $\chi_{c1}(3872) \to \gamma\psi_2(3823)$
- The largest datasets of $c\bar{c}$ vector states collected by BESIII provide the power to study the $\chi_{cJ}(1P)$, h_c states and their decays with unprecedented precision.
- Datasets above the $D\bar{D}$ threshold shed new light on charmonium-like state decays and hint at possible connections between XYZ states and the conventional charmonium.
- New data sets are currently analysed ($\sim$20fb^{-1}@$\psi(3770)$, $\sim$2.7 $\times$ 10^9@$\psi(3686)$), much more results will be presented in the future.

Thanks for your attention!

Backup

Study of the decays $\chi_{cJ} \to \Lambda\bar{\Lambda}\phi$

Significance estimation:

The significances of $\chi_{c1,2} \to \Lambda\bar{\Lambda}\phi$ are determined by comparing the difference of likelihoods with and without including each signal in the fit.

The significances of $\chi_{c0} \to \Lambda\bar{\Lambda}\phi$ are determined by another approach due to the low signal yield. We assume that the number of signal and background events in the χ_{c0} signal region follow a Poisson distribution with mean $n = s + b$, where $s = 6$ represents the expected number of signal events and $b = 0.6$ represents the expected number of background events. The p value for the null hypothesis without a resonance (H_0) is

$$p(n_{obs}) = p(n > n_{obs}|H_0) = \sum_{n>n_{obs}}^{\infty} \frac{b^n}{n!} e^{-b}$$
$$= 1 - \sum_{n=0}^{n_{obs}-1} \frac{b^n}{n!} e^{-b},$$

Where n_{obs} is the number of events observed in the signal region. The p value is obtained by calculating the probability of the number of background events fluctuating to the number of observed events in the χ_{c0} signal region. The p value is 3.89×10^{-5}, corresponding to a significance of 4.1σ. In determining this significances, the systematic uncertainties are accounted for by repeating the fits with variations of the signal shape, background shape, and fit range.

Study of the decays $\chi_{cJ} \to \Lambda\bar{\Lambda}\phi$

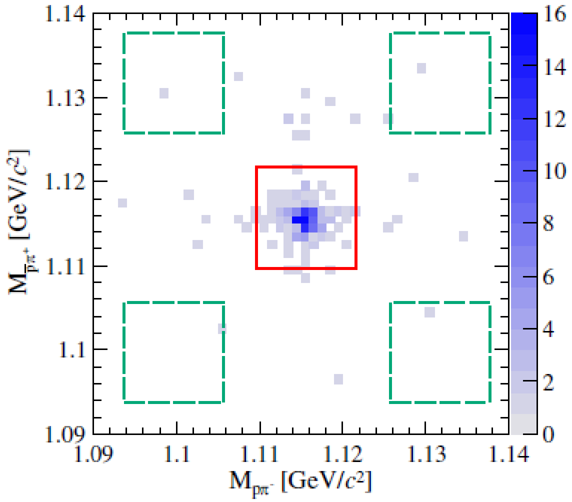

FIG. 1. The 2D distribution of $M_{\bar{p}\pi^+}$ versus $M_{p\pi^-}$ of the accepted candidates, where the box in red solid lines is the $\Lambda\bar{\Lambda}$ signal region, and the boxes in green dashed lines are the sideband regions.

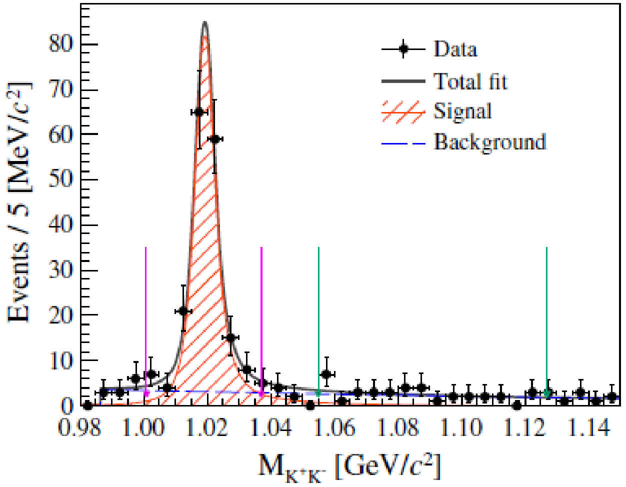

FIG. 2. Fit to the $M_{K^+K^-}$ distribution of the accepted candidates. The pink arrows show the ϕ signal region, and the pair of green arrows shows the ϕ sideband region.

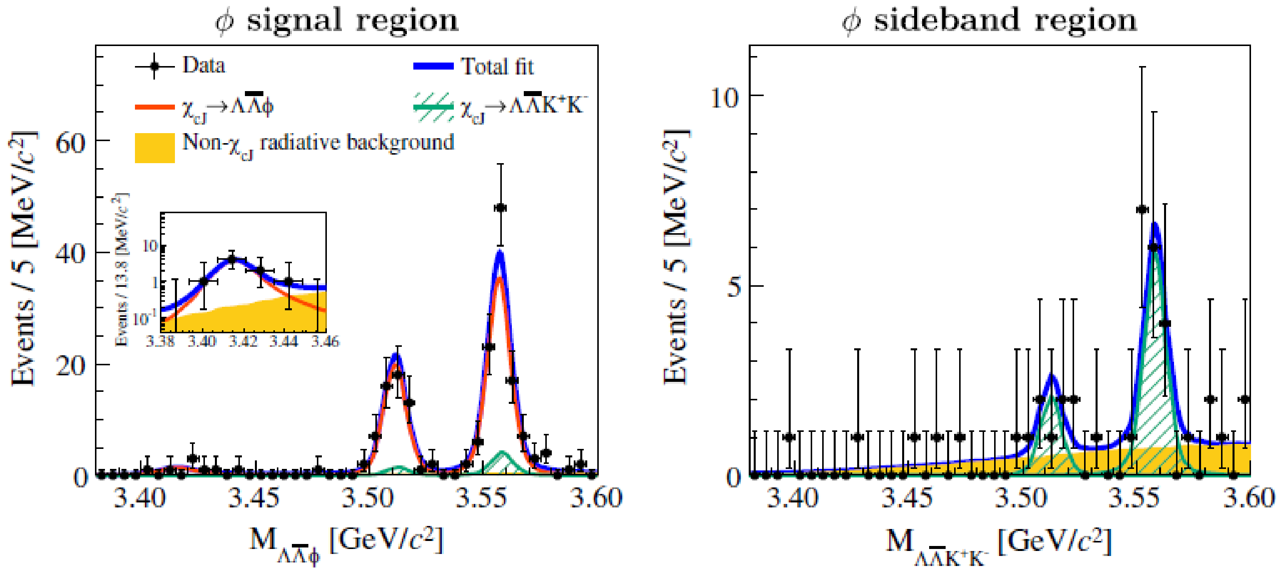

FIG. 3. Simultaneous fit to the $M_{\Lambda\bar{\Lambda}K^+K^-}$ distributions in the ϕ (left) signal and (right) sideband regions.

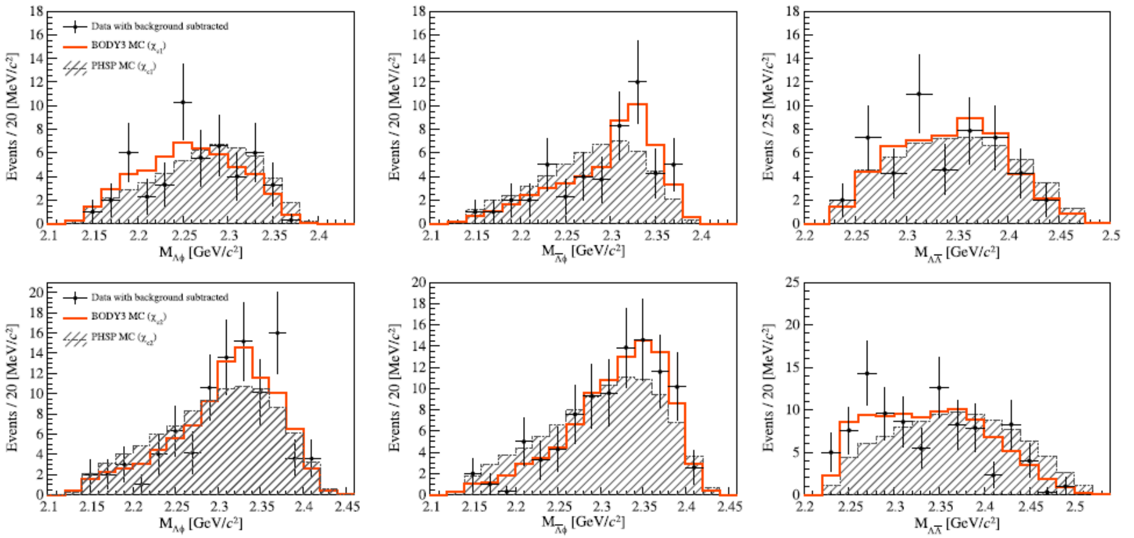

FIG. 4. Invariant-mass distributions of different two-body combinations of the decays of (top row) $\chi_{c1} \to \Lambda\bar{\Lambda}\phi$ and (bottom row) $\chi_{c2} \to \Lambda\bar{\Lambda}\phi$. The data are background subtracted. Two MC predictions are shown, one based on the PHSP model, the other on the BODY3 model.

Study of the decays $\chi_{cJ} \to \Lambda\bar{\Lambda}\omega$

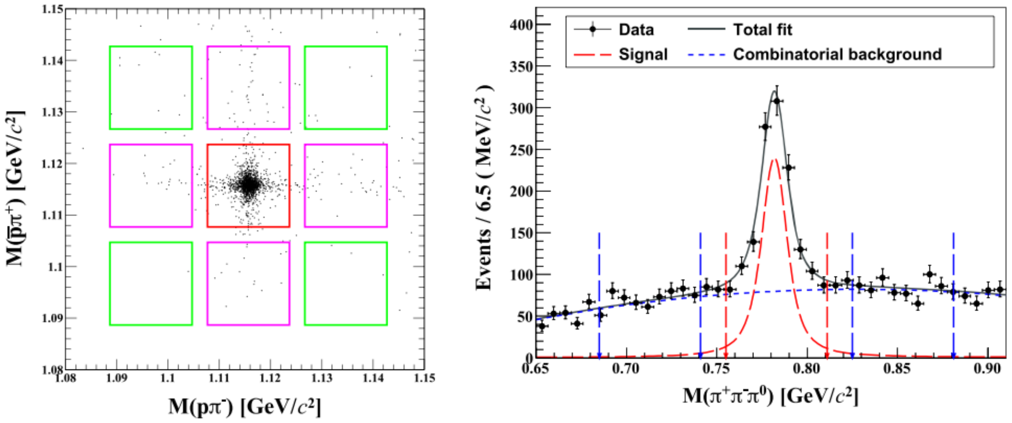

FIG. 2. The distributions of (left) $M(\bar{p}\pi^+)$ vs $M(p\pi^-)$ and (right) $M(\pi^+\pi^-\pi^0)$ of the accepted candidates. In the left figure, the central red box represents the $\Lambda\bar{\Lambda}$ signal region, the green boxes are the $\Lambda\bar{\Lambda}$ sideband region 2, and pink boxes are the $\Lambda\bar{\Lambda}$ sideband region 1. In the right figure, the red dashed line represents the fitted ω signal, and the blue dashed line denotes the combinatorial background. The gray line is the total fit. The red arrows denote the ω signal region, while the blue arrows denote the ω sideband regions.

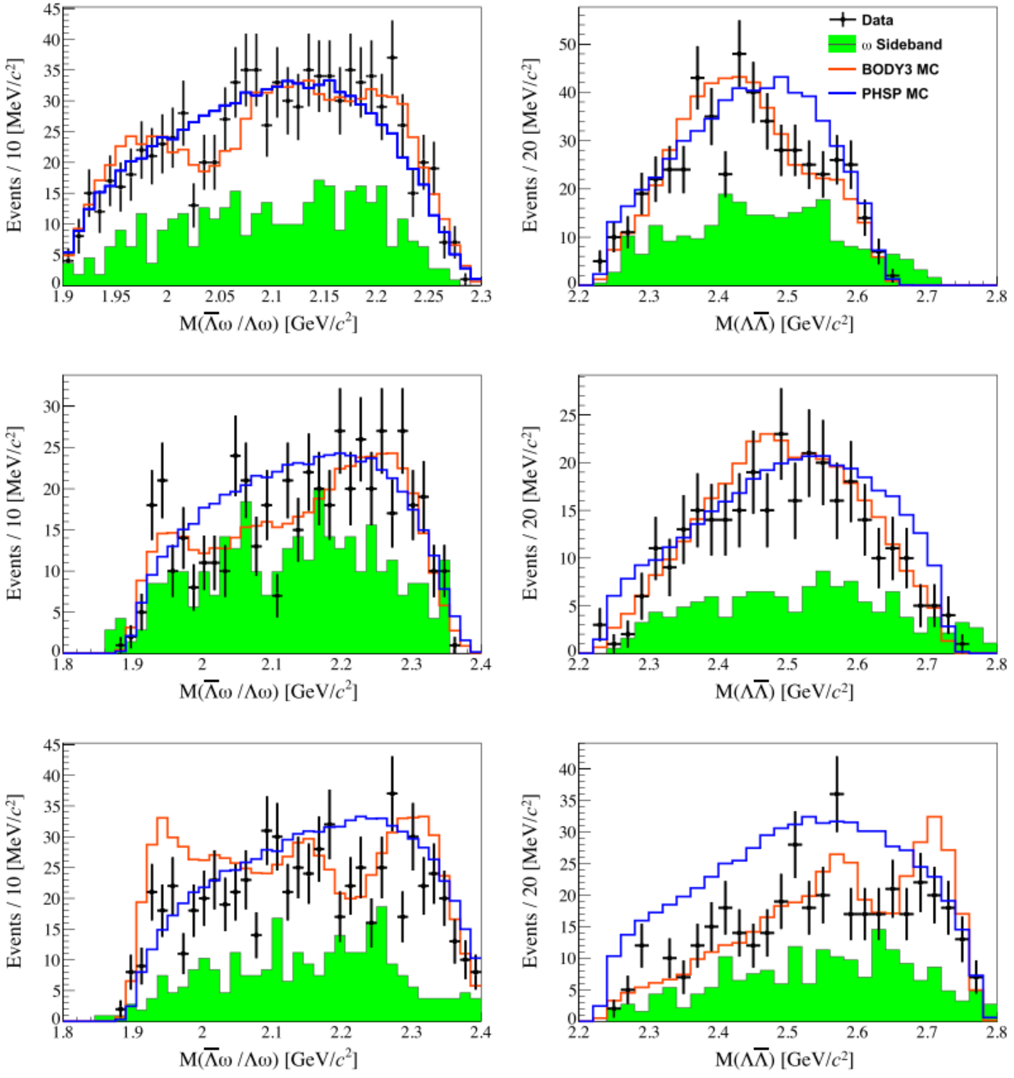

FIG. 4. Comparisons of $M(\bar{\Lambda}\omega/\Lambda\omega)$ and $M(\Lambda\bar{\Lambda})$ of (top) χ_{c0}, (middle) χ_{c1}, and (bottom) χ_{c2}, between the data and individual BODY3 signal MC samples after all event selection criteria have been applied.

Study of the decays $h_c \to \gamma\,\eta/\eta'/\pi^0$

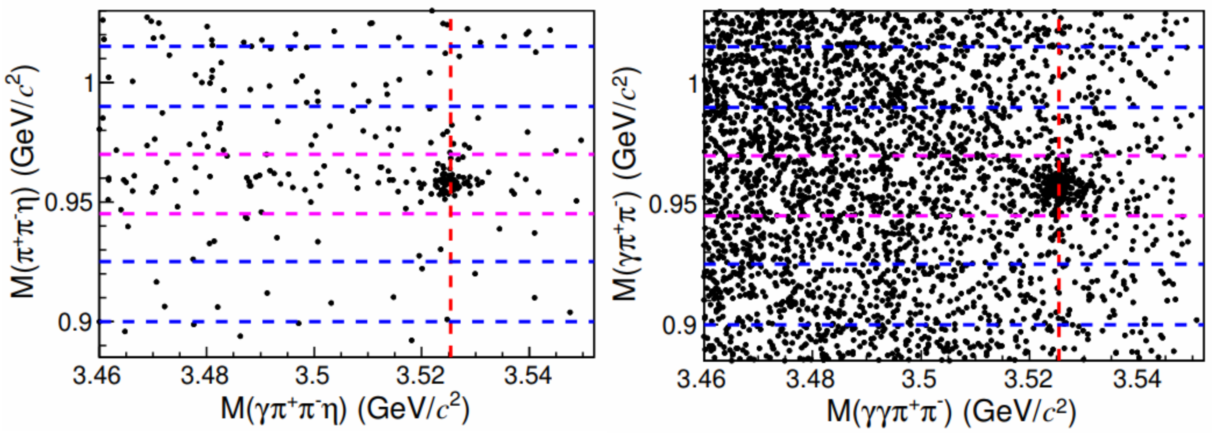

η' decay mode

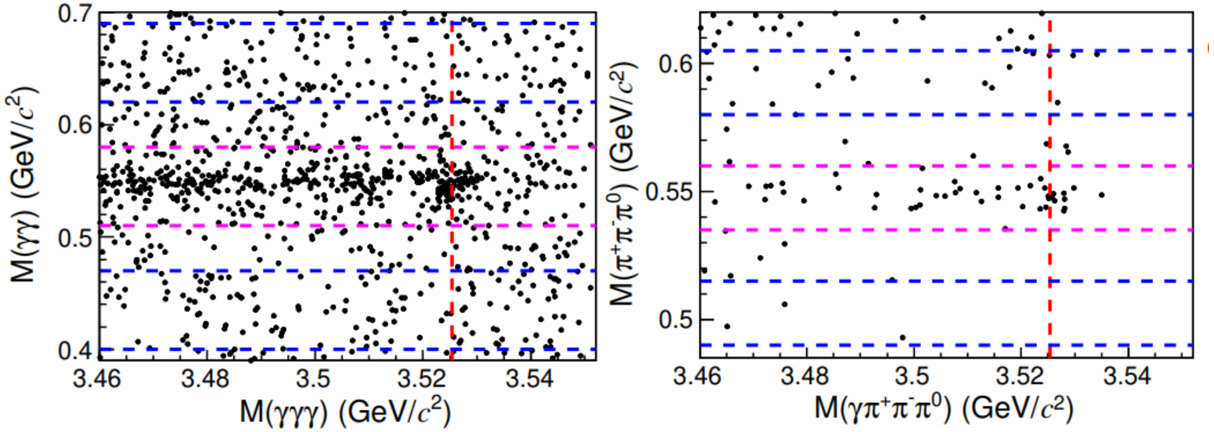

η decay mode

Source	$\eta' \to \pi^+\pi^-\eta$	$\eta' \to \pi^+\pi^-\gamma$	$\eta \to \gamma\gamma$	$\eta \to \pi^+\pi^-\pi^0$	$\pi^0 \to \gamma\gamma$
Tracking	2.0	2.0	-	2.0	-
Photon detection	1.5	1.0	1.5	0.5	0.5
π^0 reconstruction	0.5	0.5	0.5	2.4	6.4
η mass window	1.0	-	1.0	-	-
R_E ratio and $\cos\theta_{\pi^0_1\pi^0_2}$	-	-	0.8	-	-
Kinematic fit	0.9	0.6	1.5	1.5	2.8
Signal shape	0.1		0.1		-
Background shape	0.3		2.0		-
$\mathscr{B}_{\eta',\ \eta,\ \pi^0}$	1.0		0.4		0.03
$\mathscr{B}(\psi(3686) \to \pi^0 h_c)$	6.8		6.8		6.8
Number of $\psi(3686)$ events	0.5		0.5		0.5
Sum	7.3		7.5		9.8

Table 2. Relative systematic uncertainties (%) on the branching-fraction measurements, categorised by the decay chain used to reconstruct the final state. A dash (-) indicates that the source is not relevant for that decay.

$$\mathcal{R}_{h_c} = \frac{\mathcal{B}(h_c \to \gamma\eta)}{\mathcal{B}(h_c \to \gamma\eta')} = (27.0 \pm 4.4 \pm 1.0)\%$$

Search for the decays $\chi_{c1}(3872) \to \gamma\psi_2(3823)$

$\chi_{c1}(2P)$ [1]? OR

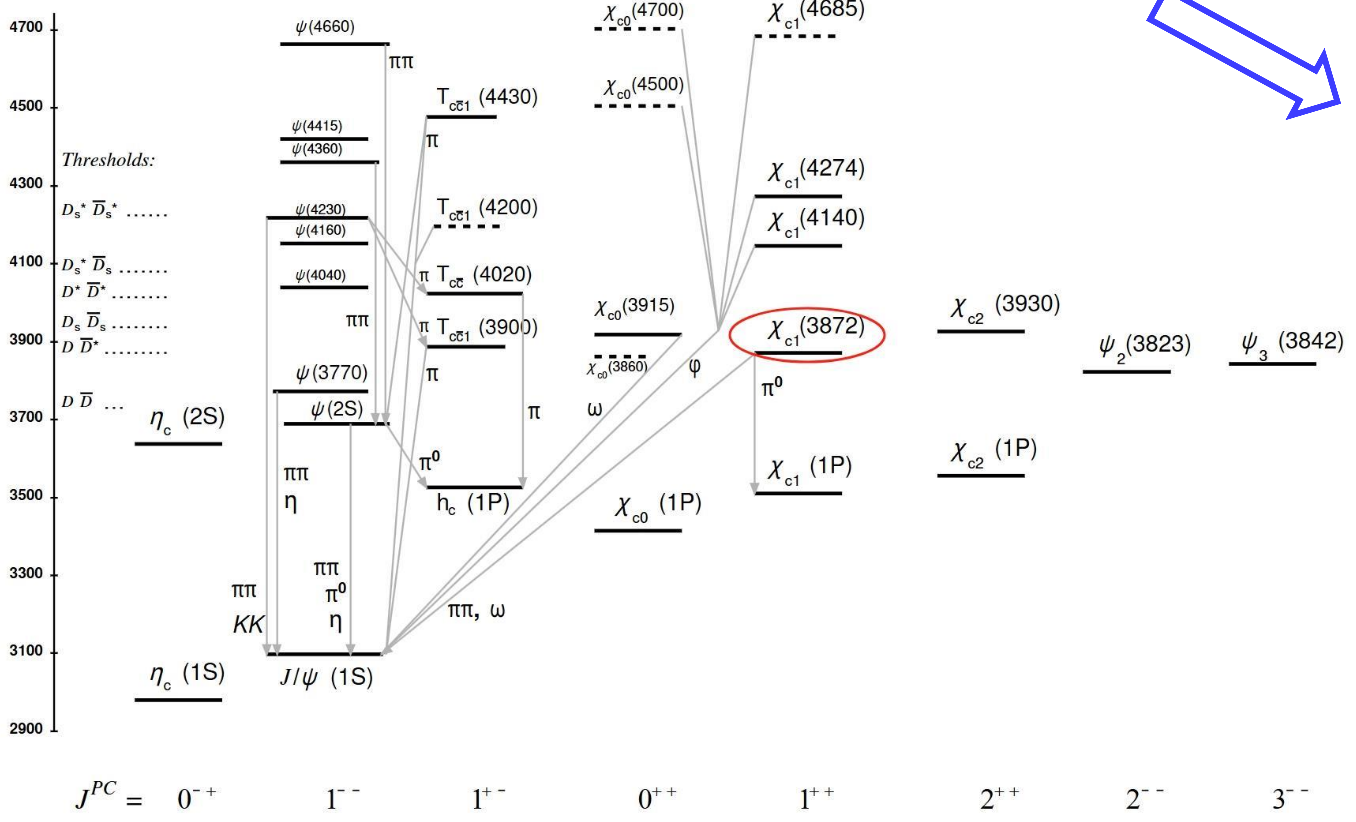

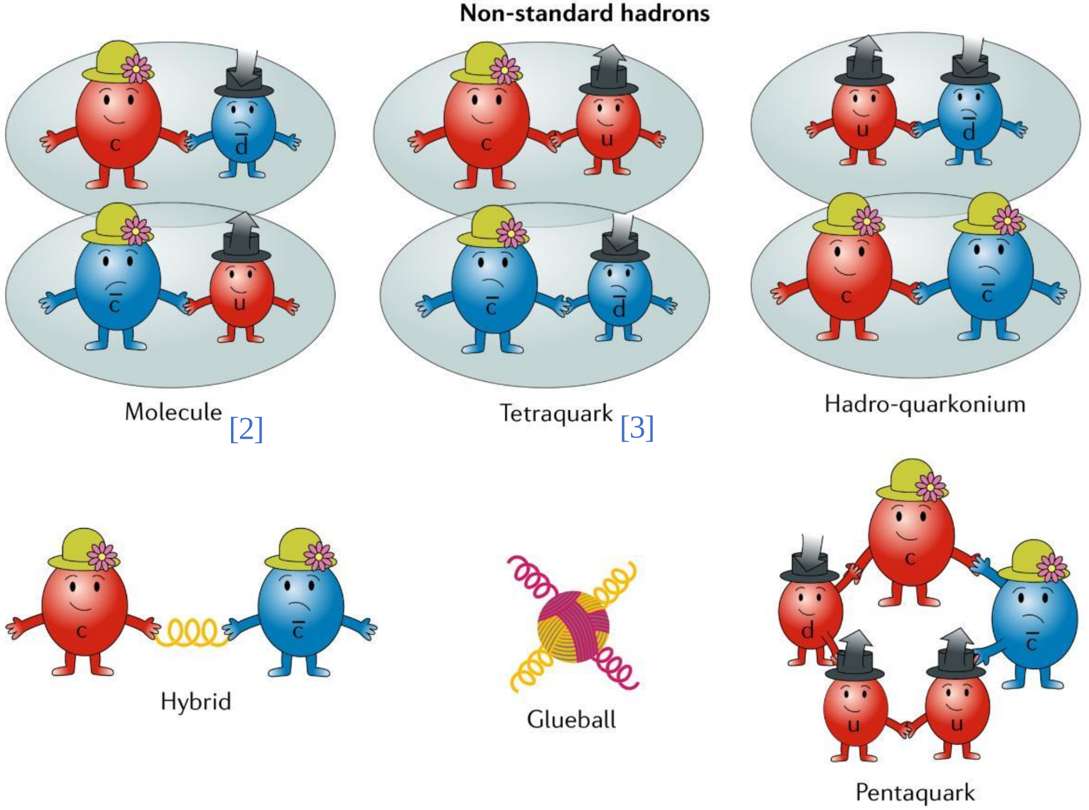

No conclusion until now!

$\chi_{c1}(3872)$

M: 3871.65 ± 0.06 MeV/c^2

Γ: 1.19 ± 0.21 MeV

$J^{pc} = 1^{++}$

[1] Phys. Rev. D **72**, 054026 (2005)
[2] Phys. Rep. **429**, 243 (2006)
[3] Phys. Rev. D **71**, 014028 (2005)

Search for the decays $\chi_{c1}(3872) \to \gamma\psi_2(3823)$

$$\chi_{c1}(3872) \to \gamma\psi_2(3823), \psi_2(3823) \to \gamma\chi_{c1}, \chi_{c1} \to \gamma J/\psi, J/\psi \to \ell^+\ell^- \ (\ell = e, \mu)$$

TABLE II. The datasets and their integrated luminosity at each energy point.

$\sqrt{s}$ (GeV)	Luminosity (pb^{-1})
4.178	3189.0
4.189	526.7
4.199	526.0
4.209	517.1
4.219	514.6
4.226	1101.0
4.236	530.3
4.244	538.1
4.258	828.4
4.267	531.1
4.278	175.7

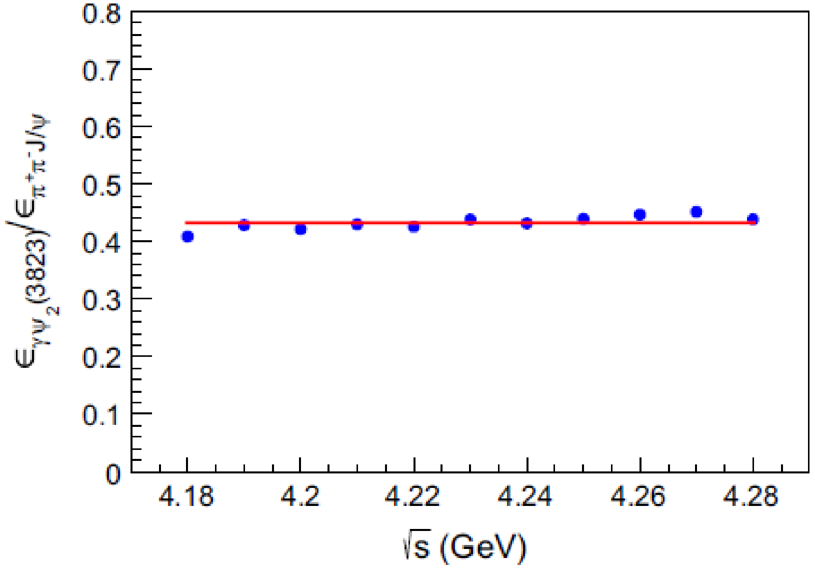

FIG. 2. Values of $\epsilon_{\gamma\psi_2(3823)}/\epsilon_{\pi^+\pi^- J/\psi}$ at each energy point (blue dots). The red line indicates the mean value.

If the $\chi_{c1}(3872)$ contains a component of the excited spin-triplet state $\chi_{c1}(2P)$, the radiative decay $\chi_{c1}(3872) \to \gamma\psi_2(3823)$ could happen naturally via an E1 transition [1], where the $\psi_2(3823)$ is considered as the 1^3D_2 charmonium state.

[1] Phys. Rev. D 72, 054026 (2005)

Search for the decays $\chi_{c1}(3872) \to \gamma\psi_2(3823)$

$$\mathcal{R}_{\chi_{c1}(3872)} = \frac{N_{obs} - r \cdot N_{obs}^{sdb}}{N_{\pi^+\pi^- J/\psi} \cdot \frac{\epsilon_{\gamma\psi_2(3823)}}{\epsilon_{\pi^+\pi^- J/\psi}} \cdot \mathcal{B}(\chi_{c1} \to \gamma J/\psi)} < 0.075$$

$N_{obs} = 0$ is the number of observed events from all data in the $\chi_{c1}(3872)$ signal region.

$N_{obs}^{sdb} = 4$ is the number of observed events in the $\chi_{c1}(3872)$ sideband region.

r is the background scaling factor.

$N_{\pi^+\pi^- J/\psi} = 80.7 \pm 9.0$ is taken from the BESIII measurements [1].

$\Gamma_{\chi_{c1}(3872)} = 1190 \pm 210$ keV [2]
$\Gamma_{\psi_2(3823)} = 520 \pm 100$ keV [3]
$\mathcal{B}(\chi_{c1}(3872) \to \pi^+\pi^- J/\psi) = (3.8 \pm 1.2) \times 10^{-2}$ [2]

	NR [4]	GI [4]	LQCD [3]
$\Gamma_{\chi_{c1}(2P)\to\gamma\psi(1^3D_2)}$ (keV)	35	18	...
$\Gamma_{\psi(1^3D_2)\to\gamma\chi_{c1}(1P)}$ (keV)	307	268	337 ± 27
$\mathcal{R}_{\chi_{c1}(2P)}$	0.46 ± 0.19	0.21 ± 0.09	0.50 ± 0.21, 0.26 ± 0.11

$\chi_{c1}(3872)$ $\Gamma: 1.19 \pm 0.21$ MeV

Γ is highly dependent on the parametrization of its line shape. This vale is from a global fit to the experimental measurements of the decay mode $\chi_{c1}(3872) \to \pi^+\pi^- J/\psi$ which describes its line shape with a BW function.

$$\Gamma_{LHCb}: 0.22^{+0.07+0.11}_{-0.06-0.13}\,\text{MeV}$$

LHCb studied the $\chi_{c1}(3872)$ line shape with a Flatté model instead [5] and determined the full width at half maximum of the line shape.

$$\Gamma_{BESIII}^{couple-channel}: 0.44^{+0.13+0.38}_{-0.35-0.25}\,\text{MeV}$$

BESIII performed a couple-channel analysis of the $\chi_{c1}(3872)$ line shape and reported a FWHM [6], consistent with the LHCb result.

If the FWHM values provided by LHCb and BESIII are used to calculate $\mathcal{R}_{\chi_{c1}(2P)}$, the ratios shown in Table will increase significantly.

Our result indicates that the $\chi_{c1}(3872)$ is not a pure $\chi_{c1}(3872)$ charmonium state.

[1] Phys. Rev. Lett. **122**, 232002 (20019)
[2] Prog. Theor. Exp. Phys. **2022**, 093C01 (2022)
[3] Phys. Rev. D **109**, 014513 (2024)
[4] Phys. Rev. D **72**, 054026 (2005)
[5] Phys. Rev. D **102**, 092005 (2020)
[6] Phys. Rev. Lett. **132**, 151903 (2024)

BEPCII-U upgrade

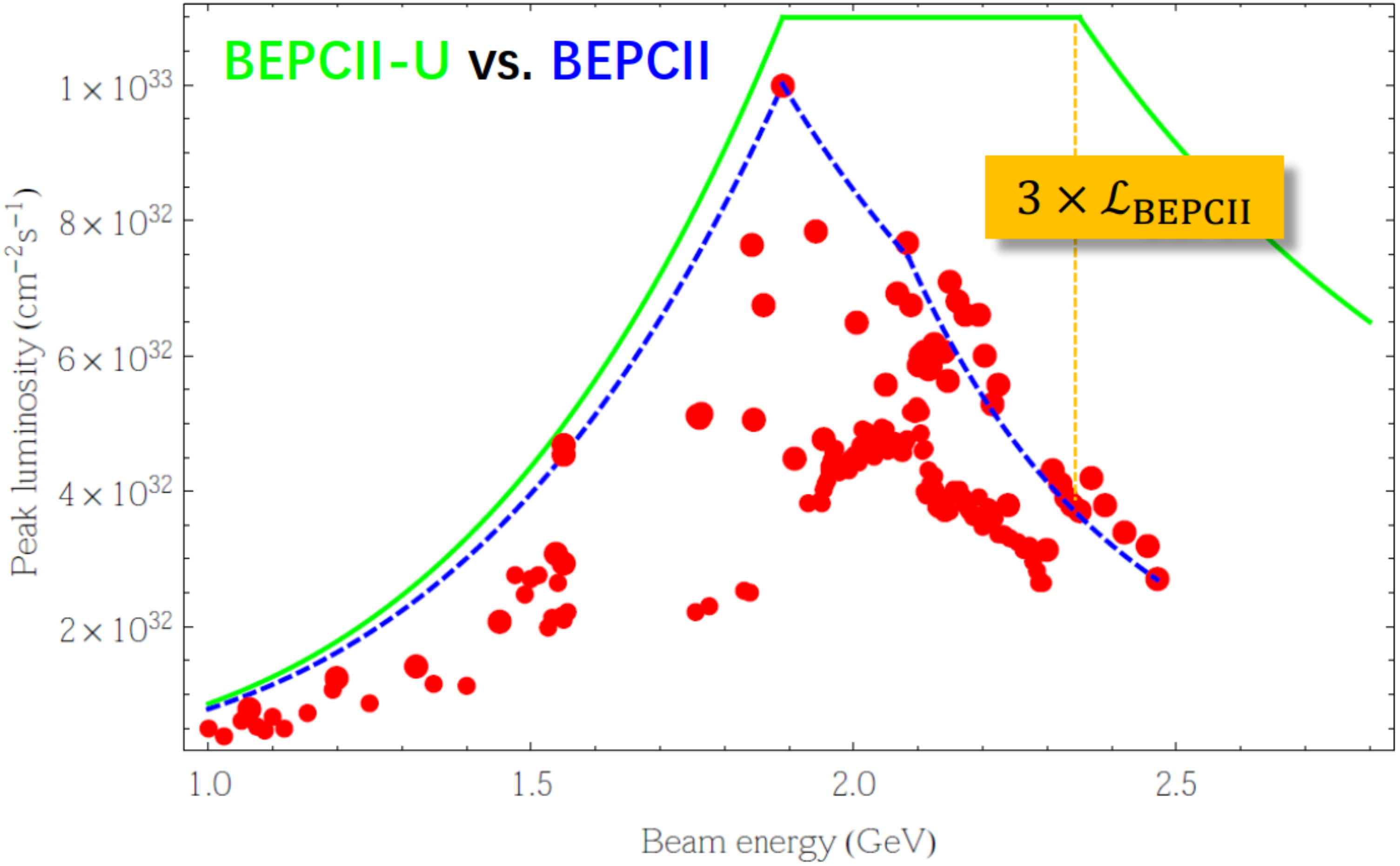

- *Luminosity increased by a factor of 3* @2.35 GeV
- *Beam energy up to* 2.8 GeV
- *Installing now, commissioning on 1ST, Jan 2025*